NOTE TO USERS

This reproduction is the best copy available.

NATURAL FREQUENCIES OF A MANIPULATOR WITH RIGID TIP MASS: THE CASE OF FLEXURAL-FLEXURAL-TORSIONAL COUPLING

By

Mohammad Arshad

B.E (Mechanical), NED University of Engineering and Technology Pakistan, December 1993

A project report

presented to Ryerson University

in partial fulfillment of the

requirement for the degree of

Master of Engineering

in the Program of

Mechanical Engineering

Toronto, Ontario, Canada, 2004

Borrower's Page

Ryerson University requires the signature of all persons using or photocopying this project report.

Please sign below, and give address and date.

Name	Address	Date

NATURAL FREQUENCIES OF A MANIPULATOR WITH RIGID TIP MASS: THE CASE OF FLEXURAL-FLEXURAL-TORSIONAL COUPLING

Mohammad Arshad

Master of Engineering, Department of Mechanical Engineering

RYERSON UNIVERSITY, Canada, 2004

Abstract

The characteristic (or frequency) equation of a flexible manipulator with a rigid tip mass is derived. The manipulator is modeled as an Euler-Bernoulli beam and it permits flexural (bending) deformation in two planes and torsional deformation. The position of the centroid of the tip mass may not necessarily be coincident with the elastic axis of the beam. This is represented by the use of offset coordinates. The natural frequencies of the manipulator are obtained by solving the characteristic equation. The results are compared to the results in the literature, where possible, and also to those obtained using a commercial finite element software ANSYS. The effects of the magnitude of the tip load, offset of the tip mass centre of gravity from its point of attachment, the length of the beam and slenderness ratio on the natural frequencies are examined.

Acknowledgments

I thank God for giving me the strength and determination to achieve my goals. I would also like to acknowledge the technical help of my project advisor, Dr. Donatus Oguamanam. I am deeply appreciative of his support and valuable advice throughout this project. I am indebted to my wife and family members for their continuous resolute support and love. Finally, I thank my colleagues for their good company and inspiration.

Table of Contents

List of Tables

List of Figures

Nomenclature

L = Length of the beam, m

A = Cross-sectional area of the beam, m^2

I = Second moment of area about the bending axis, m^4

κ^2 = Polar moment of inertia, m^4

J = Torsional constant, m^4

ρ = Density of beam material, kg/m^3

E = Modulus of elasticity, N/m^2

G = Shear modulus, N/m^2

m_t = Mass of rigid tip load, kg

I = Inertia tensor, kg.m2

$\mathcal{F}_a$ = Inertial or Newtonian dextral frame with $\hat{a}_1, \hat{a}_2$ and $\hat{a}_3$ unit vectors

$\mathcal{F}_b$ = The dextral beam body-fixed reference frame with $\hat{b}_1, \hat{b}_2$ and $\hat{b}_3$ unit vectors.

$\mathcal{F}_c$ = The dextral body-fixed reference frame with $\hat{c}_1, \hat{c}_2$ and $\hat{c}_3$ unit vectors

$\mathcal{F}_d$ =The dextral payload body-fixed reference frame with $\hat{d}_1, \hat{d}_2$ and $\hat{d}_3$ unit vectors

$\mathcal{F}_e$ = The dextral payload body-fixed reference frame with $\hat{e}_1, \hat{e}_2$ and $\hat{e}_3$ unit vectors

v (x, t) = Bending deformation (transverse displacement) in XY-plane

w (x, t) = Bending deformation (transverse displacement) in XZ-plane

φ (x, t) = Torsional deformation

ψ = Angle of rotation due to bending, rad

α = Angle of distortion due to shear, rad

k = Shear factor

o_x , o_y, o_z = Offsets of the payload centre of mass

μ^2 = Slenderness ratio

M_t = Non-dimensional payload mass

Chapter 1

1.0 Introduction

Flexural-torsional coupled vibration of a rotating structure can occur in many engineering applications such as turbo machinery blades, slewing robot arms, aircraft propellers, helicopter rotor blades, spacecraft antennae, spinning spacecraft, gun barrels and subsystems of more complex structures. To design these systems, the dynamic characteristic, especially near the resonant condition, needs to be well examined to ensure safe operation. Hence, the determination of the natural frequencies is of fundamental importance.

Flexural-torsional coupled vibration occurs when the centroidal and the shear center of the cross sections of the beam are not coincident. This lack of coincidence is observed when the beam has fewer than two axes of symmetry or has anisotropy in the material. This makes the torsional axis different from the elastic axis and thus couples torsional vibration with flexural vibration. Flexural-torsional coupled vibration is also observed in a cantilevered beam with a tip mass when the centroid of the tip mass is not coincident with the elastic axis of the beam. This is the scenario of interest in this project.

Beams are often idealized as one-dimensional structural elements. In reality, however, all structures are three-dimensional bodies with every point in the structure, if not restrained, capable of displacement along any three mutually perpendicular directions. Hence, the goal in beam models is the reduction of the various three-dimensional properties into one dimension. An exact formulation of the beam problem in terms of general elasticity equations is presented in Ref. [1]. However, it is generally difficult to solve the full problem and approximate solutions for transverse displacement are usually sufficient in most applications.

The natural frequencies of a manipulator are obtained by modeling the manipulator as a beam. The Euler–Bernoulli beam theory is assumed to be adequate to model the manipulator. The cantilevered beam is also assumed to experience small torsional deformation and planar elastic bending deformation in two directions (i.e., in XY and XZ planes, respectively) and warping effects are ignored. The centre of gravity of the rigid tip mass is not coincident with the point of attachment and Hamilton's principle is used to derive the system governing equations. A close-form expression of the characteristic (frequency) equation is derived and this is solved by using root finding techniques in MATLAB. The main advantage of a close-

form solution is that it readily highlights the "interdependencies of design variables or parameters that otherwise may not be discernable from numerical analyses" [2]. The results are compared to those in the literature and to results obtained using the ANSYS finite element software. The results show that the system natural frequency is dependent on many parameters such as magnitude of tip mass load, offset of the tip mass centre of gravity with point of attachment with beam, the length of the beam, the slenderness ratio and the bending stiffness and torsional rigidity of the beam. The results are tabulated in order to allow computational comparison and presented graphically to provide a snapshot of the influence of the abovementioned factors.

Chapter 2

2.0 Literature Review

The large amount of literature in the field of beam vibrations makes it almost impossible to list all. An attempt is, however, made here to mention the necessary and relevant articles and books in order to give an insight into the research done on the subject. In the early study of beams, bending was identified as the single most important factor in a transversely vibrating beam. This forms the basis of the Euler-Bernoulli beam theory [1]. It is the most commonly used theory because of its simplicity and its ability to provide reasonable engineering approximations to many problems. However, the theory does not provide good estimates of higher mode natural frequencies and of the natural frequencies of non-slender (i.e., thick and stout) beams, which are susceptible to shear. Other theories have been proposed to overcome these limitations. These include Rayleigh beam theory [3] and Timoshenko beam theory [4] and [5].

The Rayleigh Beam theory includes rotation effects, while the Timoshenko beam theory includes both the rotation and the shear effects. The latter gives better approximations for higher-mode responses and non-slender beams. The development and analysis of these beam theories are reviewed in the next section.

2.1 Basic Beam Theories

There are four basic beam theories: Euler-Bernoulli, Rayleigh, shear and Timoshenko beam theories. The common assumptions are

1. One dimension (the longitudinal direction) is considerably larger than the other two.
2. The material is linear elastic (Hookean).
3. The Poisson effect is neglected.
4. The cross-sectional area is symmetric so that the neutral and centroidal axes coincide.
5. The angle of rotation is small so that the small angle assumption can be used.

2.1.1 Euler-Bernoulli Beam Theory:

The simplest beam theory is the Euler-Bernoulli Beam theory which ignores both the rotary inertia and shear effects. A schematic of a cantilevered beam in transverse vibration (deflection, $v(x,t)$, is in the y direction) is shown in Fig.2.1 [6],

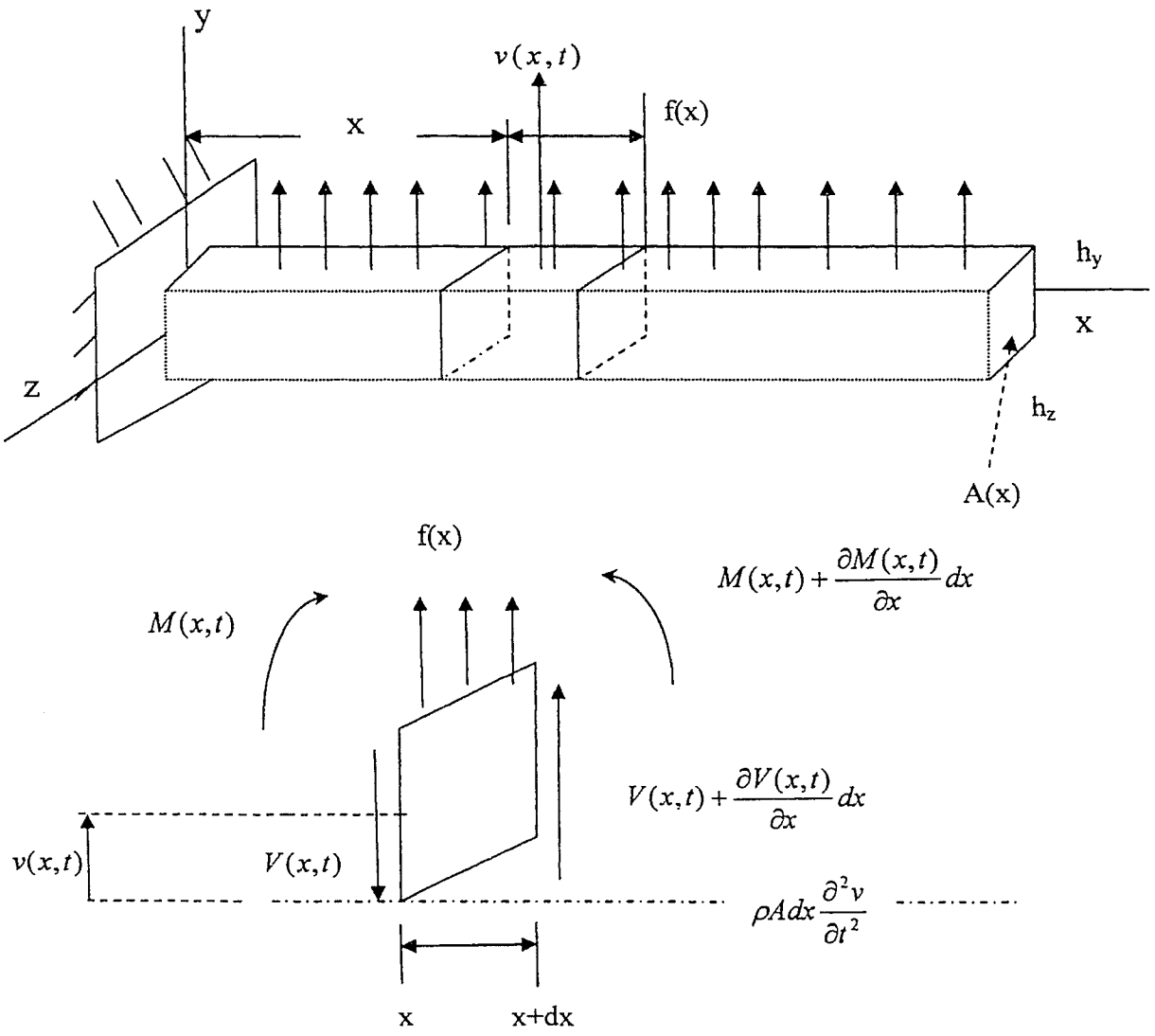

Figure 2.1: Simple beam in transverse vibration and a free-body diagram of a small element of the beam [6].

The beam is of rectangular cross section A(x) with width h_y, thickness h_z, and length L. The bending stiffness is represented by $EI(x)$, where E is the Young's modulus of elasticity and $I(x)$ is the cross-sectional area moment of inertia about the z-axis.

The strain energy of a uniform beam due to bending is

$$PE = \frac{1}{2}\int_0^L EI\left(\frac{\partial^2 v(x,t)}{\partial x^2}\right)^2 dx \tag{2.1}$$

The kinetic energy is

$$KE = \frac{1}{2}\int_0^L \rho A\left(\frac{\partial v(x,t)}{\partial t}\right)^2 dx \tag{2.2}$$

The virtual work by the transverse load is

$$\delta W = \int f(x)\delta v dx \tag{2.3}$$

where ρ and A denote the density of the beam and cross- sectional area, respectively. The Lagrangian is given as

$$\begin{aligned} L &= KE\text{-}PE \\ &= \int_0^L \left[\frac{\rho A}{2}\left(\frac{\partial v(x,t)}{\partial t}\right)^2 - \frac{EI}{2}\left(\frac{\partial^2 v(x,t)}{\partial x^2}\right)^2\right] dx \end{aligned} \tag{2.4}$$

Hamilton's principle states that the path of admissible configurations that satisfies Newton's law at each instant during the interval is the path that yields a stationary value of the time integral of the Lagrangian during the interval [7]. Therefore, extended Hamilton's principle requires that

$$\delta \int_{t1}^{t2}\int_0^L \left[\frac{\rho A}{2}\left(\frac{\partial v(x,t)}{\partial x}\right)^2 - \frac{EI}{2}\left(\frac{\partial v^2 v(x,t)}{\partial x}\right)^2 + f(x)dx\right] dxdt = 0 \tag{2.5}$$

The governing differential equation and boundary conditions are derived from the above equation by using integration by parts. The governing equation may be written as

$$\rho A\frac{\partial^2 v(x,t)}{\partial t^2} + EI\frac{\partial^4 v(x,t)}{\partial x^4} = f(x) \tag{2.6}$$

and the boundary conditions are deduced from

$$EI\frac{\partial^2 v}{\partial x^2}\delta\left(\frac{\partial v}{\partial x}\right)\Big|_0^L = 0, \tag{2.7}$$

$$EI\frac{\partial^3 v}{\partial x^3}\ \delta v\Big|_0^L = 0 \tag{2.8}$$

In regard to the physical meaning of the boundary conditions, v is the displacement, $\partial v/\partial x$ is the slope, $EI\frac{\partial^2 v}{\partial x^2}$ is the bending moment, $EI\frac{\partial^3 v}{\partial x^3}$ is the shear. The four possible combinations of end boundary conditions are

$$\begin{aligned}
&\frac{\partial^2 v}{\partial x^2} = 0, \quad \frac{\partial^3 v}{\partial x^3} = 0 && \text{free end} \\
&\frac{\partial v}{\partial x} = 0, \quad v = 0 && \text{clamped end} \\
&\frac{\partial^2 v}{\partial x^2} = 0, \quad v = 0 && \text{hinged (simply supported) end} \\
&\frac{\partial v}{\partial x} = 0, \quad \frac{\partial^3 v}{\partial x^3} = 0 && \text{sliding end}
\end{aligned} \tag{2.9}$$

2.1.2 Rayleigh Beam Model:

The Rayleigh beam theory adds rotary inertia effects to the Euler-Bernoulli beam. The Kinetic energy due to rotary inertia is

$$KE_{rot} = \frac{1}{2}\int_0^L \rho I\left(\frac{\partial^2 v(x,t)}{\partial t \partial x}\right)^2 dx \tag{2.10}$$

Therefore, the Lagrangian may be written as

$$L = \frac{1}{2}\int_0^L \left[\rho A\left(\frac{\partial v(x,t)}{\partial t}\right) + \rho I\left(\frac{\partial^2 v(x,t)}{\partial t \partial x}\right)^2 - EI\left(\frac{\partial^2 v(x,t)}{\partial x^2}\right)^2\right] \tag{2.11}$$

The use of extended Hamilton's principle yields the equation of motion as:

$$\rho A\frac{\partial^2 v(x,t)}{\partial t^2} + EI\frac{\partial^4 v(x,t)}{\partial x^4} - \rho I\frac{\partial^4 v(x,t)}{\partial x^2 \partial t^2} = f(x) \tag{2.12}$$

The boundary conditions in this case are derived from

$$EI\frac{\partial^2 v}{\partial x^2}\delta\left(\frac{\partial v}{\partial x}\right)\Big|_0^L = 0 \tag{2.13}$$

$$\left(EI\frac{\partial v^3}{\partial x^3}-\rho I\frac{\partial^3 v}{\partial x\partial t^2}\right)\delta v\Big|_0^L=0 \tag{2.14}$$

The physical meanings of the boundary conditions are that v is the displacement, $\frac{\partial v}{\partial x}$ is the slope, $EI\frac{\partial^2 v}{\partial x^2}$ is the moment, $EI\frac{\partial^3 v}{\partial x^3}-\rho I\frac{\partial^3 v}{\partial x\partial t^2}$ is the shear. The end conditions from the four combinations of boundary conditions are

$$\begin{array}{lll}
\frac{\partial^2 v}{\partial x^2}=0, \quad EI\frac{\partial^3 v}{\partial x^3}-\rho I\frac{\partial^3 v}{\partial x\,\partial t^2}=0 & & \text{free end} \\
\frac{\partial v}{\partial x}=0, \quad v=0 & & \text{clamped end} \\
\frac{\partial^2 v}{\partial x^2}=0, \quad v=0 & & \text{hinged (simply supported) end} \\
\frac{\partial v}{\partial x}=0, \quad EI\frac{\partial^3 v}{\partial x^3}-\rho I\frac{\partial^3 v}{\partial x\,\partial t^2}=0 & & \text{sliding end}
\end{array} \tag{2.15}$$

2.1.3 Shear Beam Model:

The shear beam model adds the effect of shear distortion to the Euler-Bernoulli model. It is safe to ignore the shear deformation as long as the width and thickness of the beam are small compared with the length of the beam. As the beam becomes shorter, the effects of shear deformation become evident. An element of such a beam is shown in Fig. 2.2 [6], which is a repeat of the element *dx* of Fig. 2.1 with shear deformation included.

In the figure below, the line OA is a line through the center of the element *dx* and normal to the face at the right side. The line OB, on the other hand, is the line through the tangent to the centerline of the beam. While the line OC is the centerline of the undeformed beam. The shear angle represents the effect of shear deformation. The total rotation of the cross section is the sum of the rotation due to the bending moment, ψ, and the angle of distortion due to shear, α, and it is approximated by the first derivative of deflection.

$$\psi(x,t)+\alpha(x,t)=\frac{\partial v(x,t)}{\partial x} \tag{2.16}$$

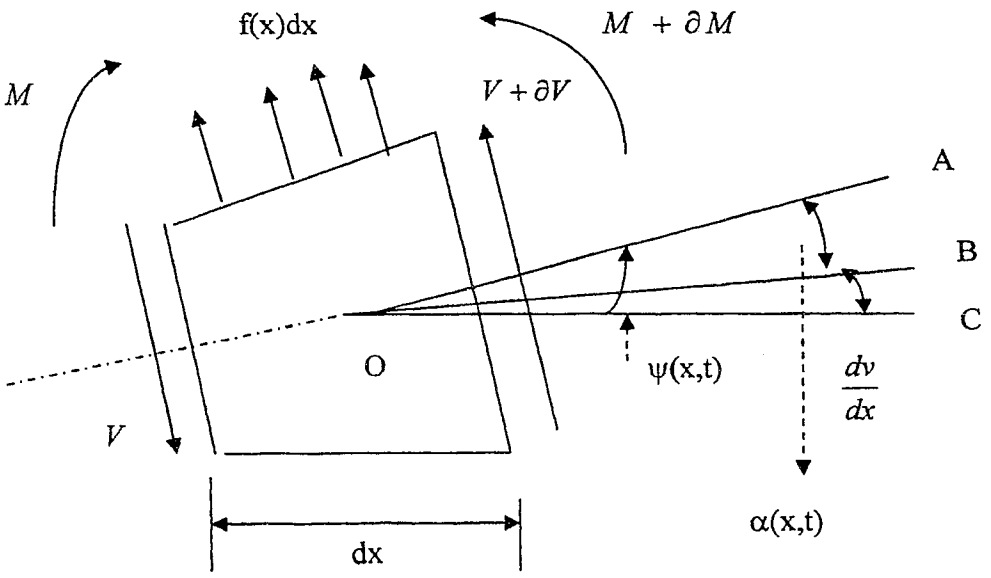

Figure 2.2: Effect of shear deformation on an element of bending beam [6].

Therefore, the strain energy resulting in bending becomes:

$$PE_{bending} = \frac{1}{2}\int_0^L \left(EI \frac{\partial \psi(x,t)}{\partial x} \right)^2 dx \tag{2.17}$$

and the strain energy resulting from shear becomes:

$$PE_{shear} = \frac{1}{2}\int_0^L kGA\left(\frac{\partial v(x,t)}{\partial x} - \psi(x,t) \right)^2 dx \tag{2.18}$$

The Lagrangian of the shear beam model is

$$L = \frac{1}{2}\int_0^L \left[\rho A\left(\frac{\partial v(x,t)}{\partial t} \right)^2 - EI\left(\frac{\partial \psi(x,t)}{\partial x} \right)^2 - kGA\left(\frac{\partial v(x,t)}{\partial x} - \psi(x,t) \right)^2 \right] dx \tag{2.19}$$

Equations of motion are obtained by Hamilton's principle and are written as:

$$\begin{aligned} \rho A \frac{\partial^2 v(x,t)}{\partial t^2} - kGA\left(\frac{\partial^2 v}{\partial x^2} - \frac{\partial \psi(x,t)}{\partial x} \right) &= f(x) \\ EI \frac{\partial^2 \psi(x,t)}{\partial x^2} + kGA\left(\frac{\partial v}{\partial x} - \psi(x,t) \right) &= 0 \end{aligned} \tag{2.20}$$

The boundary conditions are obtained from:

$$EI\frac{\partial\psi}{\partial x}\delta\psi\ \Big|_0^L = 0, \tag{2.21}$$

$$kGA\left(\frac{\partial v}{\partial x}-\psi\right)\delta v\ \Big|_0^L = 0 \tag{2.22}$$

The physical meanings are that v is the displacement and ψ is the rotation angle, $EI\frac{\partial\psi}{\partial x}$ is the bending moment, and $kGA(\partial v/\partial x-\psi)$ is the shear. The end conditions from the four possible combinations of boundary conditions

$\frac{\partial\psi}{\partial x}=0,\ kGA\left(\frac{\partial v}{\partial x}-\psi\right)=0$	free end	
$\psi=0, v=0$	clamped end	(2.23)
$\frac{\partial\psi}{\partial x}=0,\ \ v=0$	hinged (simply supported) end	
$\psi=0,\quad kGA\left(\frac{\partial v}{\partial x}-\psi\right)=0$	sliding end	

2.1.4 Timoshenko Beam Model

The Timoshenko beam model includes both shear deformation and rotatory inertia. The strain energy may be written as:

$$PE=\frac{1}{2}\int_0^L\left[EI\left(\frac{\partial\psi(x,t)}{\partial x}\right)^2+kGA\left(\frac{\partial v(x,t)}{\partial x}-\psi(x,t)\right)^2\right]dx \tag{2.24}$$

The kinetic energy includes rotatory inertia and bending motion.

$$KE=\frac{1}{2}\int_0^L\left[\rho A\left(\frac{\partial v(x,t)}{\partial t}\right)^2+\rho I\left(\frac{\partial\psi(x,t)}{\partial t}\right)^2\right]dx \tag{2.25}$$

From Eq. (2.3), the virtual work by the distributed load $f(x)$ is'

$$\delta w=\int f(x)\delta v dx$$

The Lagrangian for the Timoshenko beam becomes:

$$L=\frac{1}{2}\int_0^L\left[\rho A\left(\frac{\partial v(x,t)}{\partial t}\right)^2+\rho I\left(\frac{\partial\psi(x,t)}{\partial t}\right)^2-EI\left(\frac{\partial\psi(x,t)}{\partial x}\right)^2-kGA\left(\frac{\partial v(x,t)}{\partial x}-\psi(x,t)\right)^2\right]dx \tag{2.26}$$

The equations of motions obtained using the extended Hamilton's principles are:

$$\rho A\frac{\partial^2 v(x,t)}{\partial t^2}-kGA\left(\frac{\partial^2 v(x,t)}{\partial x^2}-\frac{\partial \psi(x,t)}{\partial x}\right)=f(x)$$
$$\rho I\frac{\partial^2 \psi(x,t)}{\partial t^2}-EI\frac{\partial^2 \psi(x,t)}{\partial x^2}-kGA\left(\frac{\partial v(x,t)}{\partial x}-\psi(x,t)\right)=0 \qquad (2.27)$$

The boundary conditions are deduced from:

$$EI\frac{\partial \psi}{\partial x}\delta\psi\ \Big|_0^L=0 \qquad (2.28)$$

$$kGA\left(\frac{\partial v}{\partial x}-\psi\right)\delta v\ \Big|_0^L=0 \qquad (2.29)$$

Note that these equations are the same as those for the shear beam model, i.e., Eq. (2.23).

The results for beam vibrations with classical boundary conditions and no attachments are presented in many standard textbooks on vibration such as Ref. [6]. The effect of end mass or tip load on the natural frequencies of beams has been investigated by numerous researchers. Goel [8] models tip load as a point mass and the beam by Euler-Bernoulli beam theory. Laura et al. [9] use the same approach and determined natural frequencies and modal shapes of a cantilevered beam which carries a finite mass at its free end.

Bruch and Mitchell [10] examine the effects of rotary inertia and shear deformation of a flexible robot arm that is modeled as a cantilever Timoshenko beam. The tip load is modeled as a rigid mass with moment of inertia about the axis of bending of the beam. They observe that the "frequencies decrease with increasing mass ratio (tip mass/beam mass) for a fixed ratio, σ (radius of gyration of the tip mass/beam length). The same is true for a fixed mass ratio and increasing σ." White and Heppler [11] generalize the study by presenting a generalized frequency equation for the Timoshenko beam. They present an exact closed form expression of the frequency equation, mode shapes and the orthogonality condition for a free–free beam with payloads at the free ends, but ignore torsional deformation and the offset of centre of gravity of payload.

Low [12] uses Euler-Bernoulli beam theory to model a rotating beam and examines the effect of hub inertia and mass load on its vibration. The natural frequencies are observed to decrease with increasing hub inertia. Oguamanam et al. [13] consider the case of a two link flexible Euler–Bernoulli beam system with one end clamped and a point mass at the free end.

Hamilton's principle is used to derive equations of motion. The frequency equation, mode shapes and the orthogonality condition are also presented along with numerical examples.

Bhat and Wagner [14] determined the natural frequencies of a uniform cantilever beam with a tip mass whose centre of gravity is not coincident with the point of attachment to the beam. This work is further extended by To [15] to include base excitation effects on natural frequencies and mode shapes. The case of a non-uniform cross-sectional beam is examined by Laura and Gutierrez [16]. Storch and Gates [17] examine transverse vibration and buckling of a cantilevered beam subjected to constant longitudinal acceleration with rigid tip mass. Two possible locations of the tip mass mass center are investigated: when the mass center is located along the beam tip tangent line, and when mass center is arbitrarily offset with respect to the beam attachment point (but not lying along the beam tip tangent line). In the former case, critical buckling loads and shapes as well as natural frequencies and mode shapes are determined analytically. Steady state solutions are shown to exist in the latter case except for certain critical values of acceleration. The free vibration problem for this latter case of tip loads is addressed in the paper.

Dokumaci [18] presents an exact determination of coupled bending and torsional vibration characteristics of uniform beams having single cross-sectional symmetry. The simplest continuous mathematical model for the analysis of coupled bending and torsion vibrations is obtained by combining the Euler-Bernoulli theory for bending and St-Venant theory for torsion. Further, it is shown that the roots of the characteristic equation of the governing differential equations of motions can be separated to obtain real exact solutions. This study is extended to include warping by Bishop et al. [19]. The inclusion of the warping effect is observed to make an appreciable difference in the results of a thin-walled beam of open section. Kirk and Wiedemann [20] use Euler-Bernoulli beam theory to determine analytical solution for the natural frequencies, mode shapes and the orthogonality condition of a free-free beam with large offset masses connected to the beam. Results are presented for different magnitudes of masses with various fixed orientations while ignoring torsional effects.

Oguamanam [2] uses Euler–Bernoulli beam theory for the determination of the natural frequencies, modal shapes and the orthogonality condition of a cantilever beam with a finite mass rigid load whose centre of gravity is not coincident with its point of attachment to the

beam. This work is extended in this project to include out-of-plane flexural deformation. The natural frequencies are calculated for a manipulator with rigid tip mass and experiencing flexural-flexural-torsional coupling. It is observed that the natural frequency is dependent on many parameters such as the magnitude of the tip mass, the offset of the tip mass centre of gravity from the point of attachment, the moments of inertia of the tip mass about the centre of gravity, the length of the beam, the slenderness ratio, and the bending stiffness and torsional rigidity of the beam.

CHAPTER 3

3.0 System Description

The flexible manipulator, modeled as a cantilever beam with a rigid tip load, is shown in Fig. 3.1. The length of the beam is denoted by L, the cross-sectional area is denoted by A, the second moment of area about the bending axis is represented by I, and the polar

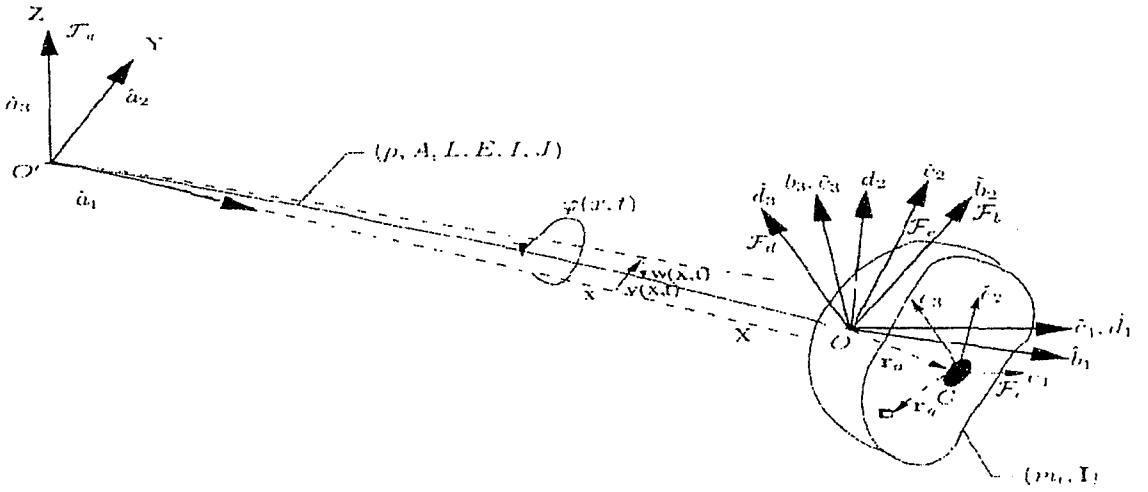

Fig.3.1 Schematic of flexible manipulator [21].

moment of inertia is denoted by J. The density, Young's modulus, and shear modulus of the beam material are respectively denoted by ρ, E, and G. The mass of the rigid tip load is denoted by M_t and its inertia tensor about the centre of gravity is represented by **I**.

The deformation of the system from its original arrangement is described by the use of five orthogonal dextral references frames which are denoted by $\mathcal{F}_a$, $\mathcal{F}_b$, $\mathcal{F}_c$, $\mathcal{F}_d$ *and* $\mathcal{F}_e$. The reference frame $\mathcal{F}_a$ is an inertial or a Newtonian frame with its origin fixed to the clamped end O' of the flexible beam. It is represented by X -, Y -, and Z-coordinate axes with the corresponding unit vectors $\hat{a}_1, \hat{a}_2$ and $\hat{a}_3$, respectively. The X-axis coincides with the longitudinal/elastic axis of the beam before deformation.

The payload is attached to the tip of the beam at point O. The dextral beam body-fixed reference frame $\mathcal{F}_b$ with unit vectors $\hat{b}_1, \hat{b}_2$ and $\hat{b}_3$ is attached to the point O in such a manner that each unit vector $\hat{b}_i$ is parallel to the corresponding $\hat{a}_i$ before deformation. The dextral body-fixed reference frame $\mathcal{F}_c$ with unit vectors $\hat{c}_1, \hat{c}_2$ and $\hat{c}_3$ is affixed to point O of the payload with each unit vector c_i parallel to the corresponding b_i. The dextral payload body-fixed reference frame $\mathcal{F}_d$ with unit vectors $\hat{d}_1, \hat{d}_2$ and $\hat{d}_3$ is attached at the point of attachment of the payload. The fifth dextral payload body-fixed reference frame $\mathcal{F}_e$ having unit vectors $\hat{e}_1, \hat{e}_2$ and $\hat{e}_3$ is attached to the centre of gravity of the payload and all its unit vectors are always parallel to the corresponding unit vectors of reference frame $\mathcal{F}_d$.

The position vector from the point of attachment of the payload O to the centre of gravity of the payload G is denoted by r_o and it has the Cartesian components o_x, o_y, and o_z. A differential beam element located at position (x,y) from the clamped end O' of the beam is assumed to experience both torsional deformation φ (x, t) and bending deformations v(x, t) and w(x, t) in the XY plane and the XZ plane, respectively.

3.1 The System Governing Equations:

The governing equations and boundary conditions of the system are derived in [21], and these are presented below:

Equations of motion:

$$\rho A\ddot{v} + EI_{yy}^{B} v''' = 0 \tag{3.1}$$

$$\rho A\ddot{w} + EI_{yy}^{B} w''' = 0 \tag{3.2}$$

$$\rho \kappa^2 \ddot{\varphi} - GJ\varphi'' = 0 \tag{3.3}$$

and boundary conditions

$$v(0,t) = v'(0,t) = 0 \tag{3.4}$$

$$m_t \ddot{v}(L,t) + m_t o_x \ddot{v}'(L,t) + m_t o_z \ddot{\varphi}(L,t) - EI_{zz}^{B} v'''(L,t) = 0 \tag{3.5}$$

$$m_t o_x \ddot{v}(L,t) + (I_{zz} + m_t(o_x^2 + o_y^2))\ddot{v}'(L,t) + (I_{xz} + m_t o_x o_z)\ddot{\varphi}(L,t) +$$
$$(I_{yz} + m_t o_y o_z)\ddot{w}'(L,t) + EI_{yy}^{B} v''(L,t) = 0 \tag{3.6}$$

$$w(0,t) = w'(0,t) = 0 \tag{3.7}$$

$$m_t \ddot{w}(L,t) + m_t o_x \ddot{w}'(L,t) - m_t o_y \ddot{\varphi}(L,t) - EI_{yy}^{B} w'''(L,t) = m_t g \tag{3.8}$$

$$m_t o_x \ddot{w}(L,t) + (I_{yy} + m_t(o_x^2 + o_z^2))\ddot{w}'(L,t) + (I_{xy} - m_t o_x o_y)\ddot{\varphi}(L,t) +$$
$$(I_{yz} + m_t o_y o_z)\ddot{v}'(L,t) + EI_{yy}^{B} w''(L,t) = m_t g o_x \tag{3.9}$$

$$\varphi(0,t) = 0 \tag{3.10}$$

$$m_t o_z \ddot{v}(L,t) - m_t o_y \ddot{w}(L,t) + (I_{xx} + m_t(o_y^2 + o_z^2))\ddot{\varphi}(L,t) +$$
$$(I_{xz} + m_t o_x o_z)\ddot{v}'(L,t) + (I_{xy} - m_t o_x o_y)\ddot{w}'(L,t) +$$
$$GJ\varphi'(L,t) = -m_t g o_y \tag{3.11}$$

Where $(\,)' = \frac{\partial}{\partial x}$ and $(\dot{}) = \frac{\partial(\,)}{\partial t}$

The above governing equations Eqs. (3.1)–(3.3) are uncoupled, but the system dynamics are coupled via the boundary conditions. The method of separation of variables can not be used to solve these equations because of the presence of non-homogeneous boundary conditions. Homogeneity can be ensured by introducing new variables γ and w_*, which are defined as

$$\gamma(x,t) = \varphi - \frac{m_t g}{GJ} o_y x \tag{3.12}$$

$$w_*(x,t) = w(x,t) - \frac{m_t g}{2EI_{yy}^B} x^2 (o_x + L) + \frac{m_t g}{6EI_{yy}^B} x^3 \tag{3.13}$$

For ease of analysis and presentation, the following non-dimensional parameters are introduced.

$$\xi = \frac{x}{L}, \quad a_i = \frac{o_i}{L} \; i \in \{x,y,z\}, \quad \lambda_1^4 = \frac{\rho A L^4 w^2}{EI_{yy}^B}, \quad \lambda^4 = \frac{\rho A L^4 w^2}{EI_{zz}^B} \tag{3.14}$$

$$\alpha^4 = \frac{I_{zz}^B}{I_{yy}^B} \quad \chi^2 = \frac{EI_{zz}^B}{GJ}, \quad \mu^2 = \frac{\kappa^2}{AL^2} \quad M_t = \frac{m_t}{\rho AL}, \quad \mathrm{I}_{ij} = \frac{I_{ij}}{\rho AL^3} \quad i,j \in \{x,y,z\}$$

The separable solutions are assumed in the forms:

$$v(x,t) = LV(\xi)e^{iwt}, \; w_*(x,t) = LW_*(\xi)e^{iwt} \text{ and } \gamma(x,t) = \Gamma(\xi)e^{iwt} \tag{3.15}$$

Equation (3.15), in conjunction with Eqs. (3.12)-(3.14), is substituted into Eqs. (3.1)-(3.11) to obtain the following non-dimensional system governing equations

$$V'''' - \lambda^4 V = 0 \tag{3.16}$$

$$W_*'''' - \lambda^4 \alpha^4 W_* = 0 \tag{3.17}$$

$$\Gamma'' - \lambda^4 \mu^2 \chi^2 \Gamma = 0 \tag{3.18}$$

which are subjected to the following boundary conditions:

$$V(0) = V'(0) = 0 \tag{3.19}$$

$$\lambda^4 M_t (V(1) + a_x V'(1) + a_z \Gamma(1)) + V'''(1) = 0 \tag{3.20}$$

$$\chi^4\{M_t a_x(V(1)_{zz} + M_t(a_x^2 + a_y^2))V'(1) + (I_{xz} + M_t a_x a_z)\Gamma(1) +$$

$$(I_{yz} + M_t a_y a_z)W_*'(1)\} - V''(1) = 0 \qquad (3.21)$$

$$W_*(0) = W_*'(0) = 0 \qquad (3.22)$$

$$\chi^4\alpha^4 M_t(W_*(1) + a_x W_*'(1) - a_y\Gamma(1)) + W_*''' = 0 \qquad (3.23)$$

$$\chi^4\alpha^4\{M_t a_x W_*(1) + (I_{yy} + M_t(a_x^2 + a_y^2))W_*'(1) + (I_{xy} - M_t a_x a_y)\Gamma(1) +$$

$$(I_{yz} + M_t a_y a_z)V'(1)\} - W_*''(1) = 0 \qquad (3.24)$$

$$\Gamma(0) = 0 \qquad (3.25)$$

$$\chi^4\chi^2\{M_t a_z V(1) - M_t a_y W_*(1) + (I_{xx} + M_t(a_y^2 + a_z^2))\Gamma(1) +$$

$$(I_{xz} + M_t a_x a_z)V'(1) - (I_{xy} - M_t a_x a_y)W_*'(1)\} - \Gamma'(1) = 0 \qquad (3.26)$$

Chapter 4

4.0 Characteristic Equation

Taking into consideration the boundary conditions, Eqs.(3.19) and (3.25), the general solution to the governing equations (i.e., Eqs. (3.16)- (3.18)) can be written as

$$V(\xi) = A_1(\sin(\lambda\xi) - \sinh(\lambda\xi)) + A_2(\cos(\lambda\xi) - \cosh(\lambda\xi)) \tag{4.1}$$

$$W.(\xi) = B_1(\sin(\lambda\xi) - \sinh(\lambda\xi)) + B_2(\cos(\lambda\xi) - \cosh(\lambda\xi)) \tag{4.2}$$

$$\Gamma(\xi) = C\sin(\lambda^2\chi\mu\xi) \tag{4.3}$$

The above equations are substituted into the remaining boundary conditions Eqs. (3.20),(3.21),(3.23),(3.24) and (3.26)) to yield a set of equations that is expressed by using compact matrix notation as

$$A_{5\times5}X_{5\times1} = 0 \tag{4.4}$$

Where $X=[C\ A_1\ A_2\ B_1\ B_2]^T$ is column vector of the coefficients of the general solutions, Eqs. (4.1)-(4.3). The frequency (or characteristic) equation is obtained by equating the determinant of matrix A in Eq. (4.4) to zero; it may be written as

$$(\mu c_u F_{cfv} - \lambda^2\chi I_{xxt} s_u F_{cfv} - \lambda^3\mu I_{zzt} c_u F_{crv} + \lambda^5\chi s_u (I_{xxt} I_{zzt} - I_{xzt}^2) F_{crv}) F_{cfw} -$$

$$\lambda^3\alpha^3(\mu c_u I_{yyt} F_{cfv} - \lambda^2\chi s_u (I_{xxt} I_{yyt} - I_{xyt}^2) F_{cfv} - \lambda^3\mu c_u I_{yyt} I_{zzt} F_{crv} +$$

$$\lambda^5\chi s_u (I_{xxt} I_{yyt} I_{zzt} - I_{yyt} I_{xzt}^2 - I_{xyt}^2 I_{zzt}) F_{cfv} + I_{xyt} I_{xzt} I_{yzt}) F_{crv}) F_{crw} -$$

$$M_t[\lambda(\mu c_u F_{csv} + 2\lambda\mu a_x c_u s_v sh_v - \lambda^2\chi I_{xxt} s_u F_{csv} - \lambda^3\mu I_{zzt} c_u F_{ccv} + 2\lambda^3\chi s_u (a_z I_{xzt} -$$

$$a_x I_{xxt}) s_v sh_v + \lambda^5\chi s_u (I_{xxt} I_{zzt} - I_{xzt}^2) F_{ccv}) + \lambda\alpha(\mu c_u F_{csw} + 2\lambda\alpha\mu a_x c_u s_w sh_w -$$

$$\lambda^2\chi I_{xxt} s_u F_{csw} - \lambda^3\alpha^3\mu I_{yyt} c_u F_{ccw} - 2\lambda^3\alpha\chi s_{1u} (a_y I_{xyt} + a_x I_{xxt}) s_w sh_w +$$

$$\lambda^5\alpha^3\chi s_u (I_{xxt} I_{yyt} - I_{xyt}^2) F_{ccw}) F_{cfv} + \lambda^4\alpha^3(\lambda^3(\chi s_u s_v sh_v (2a_x (I_{xxt} I_{yyt} - I_{xyt}^2) -$$

$$a_z (2I_{xzt} I_{yyt} - I_{yzt} I_{xyt})) + \mu c_u I_{yyt} I_{zzt} F_{ccv} + \lambda^2\chi s_u (I_{xxt} I_{yyt} - I_{xyt}^2) F_{csv} -$$

$$\mu c_u I_{yyt} (F_{csv} + 2\lambda a_x s_v sh_v)) F_{crw} + \lambda^4\alpha(\chi s_u s_w sh_w (2a_x (I_{xxt} I_{zzt} - I_{xzt}^2) +$$

$$a_y(2I_{xyt}I_{zzt} - I_{xzt}I_{yzt})) + \alpha^2\mu c_u I_{yyt}I_{zzt}F_{ccw}) + \lambda^2\chi s_u(I_{xxt}I_{zzt} - I_{xzt}^2)F_{csw} -$$

$$\mu c_u I_{zzt}(F_{csw} + 2\lambda\alpha a_x s_w sh_w))F_{crv} + \lambda^9\alpha^3\chi s_u(I_{xxt}I_{yyt}I_{zzt} - I_{yyt}I_{xzt}^2 - I_{xyt}^2 I_{zzt} +$$

$$I_{xyt}I_{xzt}I_{yzt})(F_{ccv}F_{crw} + \alpha F_{crv}F_{ccw})] -$$

$$M_t^2[\lambda^3(\chi a_z^2 s_u F_{csv} + \lambda\mu a_x^2 c_u F_{ccv} - \lambda^3\chi s_u(a_x^2 I_{xxt} - 2a_x a_z I_{xzt} + a_z^2 I_{zzt})F_{ccv})F_{cfw} +$$

$$\lambda^3\alpha(\chi a_y^2 s_u F_{csw} + \lambda\alpha^3\mu a_x^2 c_u F_{ccw} - \lambda^3\alpha^3\chi s_u(a_x^2 I_{xxt} + 2a_x a_y I_{xyt} + a_y^2 I_{yyt})F_{ccw})F_{cfv} +$$

$$\lambda^4\alpha^2 s_v sh_v s_w sh_w(\lambda^2\chi s_u(4a_x(a_x I_{xxt} + a_y I_{xyt} - a_z I_{xzt}) - a_y a_z I_{yzt}) - 4\mu a_x^2 c_u) -$$

$$\lambda^2\alpha\mu c_u(F_{csv}F_{csw} + 2\lambda a_x(s_v sh_v F_{csw} + \alpha s_w sh_w F_{csv})) + \lambda^4\alpha\chi s_u(F_{csv}F_{csw} + 2\lambda a_x(s_v sh_v F_{csw} +$$

$$\alpha s_w sh_w F_{csv}))I_{xxt} + \lambda^5\alpha^3(\mu\alpha c_u(F_{csv} + 2\lambda a_x s_v sh_v)F_{ccw} - \lambda(\lambda\mu a_x^2 c_u F_{ccv} + \chi a_z^2 s_u F_{csv})F_{crw})I_{yyt} +$$

$$\lambda^5\alpha(\mu c_u(F_{csw} + 2\lambda\alpha a_x s_w sh_w)F_{ccv} - \lambda(\lambda\alpha^3\mu a_x^2 c_u F_{ccw} + \chi a_y^2 s_u F_{csw})F_{crv})I_{zzt} +$$

$$2\lambda^5\alpha\chi s_u(\alpha a_y s_w sh_w F_{csv}I_{xyt} - a_z s_v sh_v F_{csw}I_{xzt}) - \lambda^7\alpha^3\chi s_u(\alpha F_{csv}F_{ccw} - \lambda a_x(\lambda a_x F_{ccv}F_{crw} -$$

$$2\alpha s_v sh_v F_{ccw}))(I_{xxt}I_{yyt} - I_{xyt}^2) - \lambda^7\alpha\chi s_u(F_{ccv}F_{csw} - \alpha\lambda a_x(\lambda\alpha^2 a_x F_{crv}F_{ccw} -$$

$$2s_w sh_w F_{ccv}))(I_{xxt}I_{zzt} - I_{xzt}^2) - \lambda^8\alpha^3\chi a_z s_u(\alpha s_v sh_v F_{ccw} - \lambda a_x F_{ccv}F_{crw})(I_{xyt}I_{yzt} - 2I_{xzt}I_{yyt}) +$$

$$\lambda^8\alpha^2\chi a_y s_u(s_w sh_w F_{ccv} - \lambda\alpha^2 a_x F_{crv}F_{ccw})(I_{xzt}I_{zzt} - 2I_{xyt}I_{zzt}) - \lambda^8\alpha^3(\alpha\mu c_u F_{ccv}F_{ccw} -$$

$$\lambda\chi s_u(\alpha a_y^2 F_{crv}F_{crw} + a_z^2 F_{ccv}F_{crw}))I_{yyt}I_{zzt} + \lambda^{10}\alpha^4\chi s_u F_{ccv}F_{ccw}(I_{xxt}I_{yyt}I_{zzt} - I_{xzt}^2 I_{yyt} -$$

$$I_{xyt}^2 I_{zzt} + I_{xyt}I_{xzt}I_{yzt})] -$$

$$\lambda^4\alpha M_t^3[-\lambda\mu a_x^2 c_u(F_{csw} + 2\lambda\alpha a_x s_w sh_w)F_{ccv} - \chi a_y^2 s_u(F_{csv} + 2\lambda a_x)F_{csw} -$$

$$\lambda\alpha^3\mu a_x^2 c_u(F_{csv} + 2\lambda a_x s_v sh_v)F_{ccw} - \chi a_z^2 s_u(F_{csw} + 2\lambda\alpha a_x)F_{csw} +$$

$$\lambda^3\chi a_x^2 s_u((F_{ccv}F_{csw} + \alpha^3 F_{csv}F_{ccw}) + 2\lambda\alpha a_x(s_w sh_w F_{ccw} + \alpha^2 s_v sh_v F_{ccw}))I_{xxt} +$$

$$\lambda^3\alpha^2(\lambda\mu a_x^2 c_u + \chi s_u(a_y^2 + a_x^2)F_{csv} + 2\lambda\chi a_x a_y^2 s_u s_v sh_v)F_{ccw}I_{yyt} +$$

$$\lambda^3(\lambda\alpha^3\mu a_x^2 c_u F_{ccw} + \chi s_u(a_y^2 + a_z^2)F_{csw} + 2\lambda\alpha\chi a_x a_z^2 s_u s_w sh_w)F_{ccv}I_{zzt} +$$

$$2\lambda^3\alpha\chi a_x a_y s_u((\alpha^2 F_{csv} + 2\lambda a_x s_v sh_v)F_{ccw} + \lambda a_x s_w sh_w F_{ccv})I_{yzt} -$$

$$2\lambda^3\chi a_x a_z s_u((F_{csw} + 2\lambda\alpha a_x s_w sh_w)F_{ccw} + \lambda\alpha^3 a_x s_v sh_v F_{ccw})I_{zzt} -$$

$$\lambda^4\alpha\chi a_x a_y a_z s_u (s_w sh_w F_{ccv} + \alpha^2 s_v sh_v F_{ccw}) \mathrm{I}_{yzt} +$$

$$\lambda^6\alpha^3\chi s_u (a_x^2(\mathrm{I}_{xyt}^2 + \mathrm{I}_{xzt}^2 - \mathrm{I}_{xxt}\mathrm{I}_{zzt} - \mathrm{I}_{xxt}\mathrm{I}_{yyt}) - a_x a_z(\mathrm{I}_{xyt}\mathrm{I}_{yzt} - 2\mathrm{I}_{yyt}\mathrm{I}_{xzt}) +$$

$$a_x a_y(\mathrm{I}_{xzt}\mathrm{I}_{yzt} - 2\mathrm{I}_{xyt}\mathrm{I}_{zzt}))F_{ccv}F_{ccw}] +$$

$$\lambda^7\alpha a_x^2 M_t^4[\lambda\mu\alpha^3 a_x^2 c_u F_{ccv}F_{ccw} + a_y^2\chi s_u F_{ccv}F_{csw} + \alpha^3\chi a_z^2 s_u F_{csv}F_{ccw} -$$

$$\lambda^3\alpha^3\chi s_u(a_x^2\mathrm{I}_{xxt} + a_y^2\mathrm{I}_{yyt} + a_z^2\mathrm{I}_{zzt} + 2a_x a_y\mathrm{I}_{xyt} - 2a_x a_z\mathrm{I}_{xzt} - a_y a_z\mathrm{I}_{yzt})F_{ccv}F_{ccw}] = 0 \quad (4.5)$$

where

$$F_{cf\beta} = 1 + c_\beta ch_\beta,\quad F_{cr\beta} = s_\beta ch_\beta + c_\beta sh_\beta,\quad F_{cs\beta} = s_\beta ch_\beta - c_\beta sh_\beta,\quad F_{cc\beta} = 1 - c_\beta ch_\beta$$

$$s_u = \sin(\lambda^2\chi\mu),\ s_v = \sin(\lambda\alpha),\ c_v = \cos(\lambda), sh_v = \sinh(\lambda), ch_v = \cosh(\lambda)$$

$$c_u = \cos(\lambda^2\chi\mu),\ s_w = \sin(\lambda\alpha)\ , c_w = \cos(\lambda\alpha), sh_w = \sinh(\lambda\alpha), ch_w = \cosh(\lambda\alpha)$$

$$I_{xxt} = I_{xx} + M_t(a_y^2 + a_z^2),\ I_{yyt} = I_{yy} + M_t(a_x^2 + a_z^2),\ I_{zzt} = I_{zz} + M_t(a_x^2 + a_y^2)$$

$$I_{xyt} = -M_t a_x a_y\ ,\ I_{xzt} = M_t a_x a_z\ ,\ I_{yzt} = M_t a_y a_z \text{ and } \beta\ \varepsilon\ \{v, \varpi\}$$

If the bending rigidity in the y-axis is very large compared with that in the z-axis. (i.e., $\alpha \to 0$) which implies that $F_{cfw} \to 2$ and $F_{ccw} \to F_{crw}$, and $F_{csw\to 0}$, the frequency equation Eq.(4.5) reduces to:

$$\mu c_{1u}F_{cf} - \lambda^2\chi I_{xxt}s_{1u}F_{cf} - \lambda^3\mu I_{zzt}c_{1u}F_{cr} + \lambda^5\chi s_{1u}(I_{xxt}I_{zzt} - I^2{}_{xzt})F_{cr} - M_t[\lambda\mu c_{1u}F_{cs}$$
$$+ 2\lambda^2\mu a_x c_{1u}s_1 sh_1 - \lambda^3\chi I_{xxt}s_{1u}F_{cs} - \lambda^4\mu I_{zzt}c_{1u}F_{cc} + 2\lambda^4\chi s_{1u}(a_z I_{xzt} - a_x I_{xxt})s_1 sh_1 -$$
$$+ \lambda^6\chi s_{1u}(I_{xxt}I_{zzt} - I^2{}_{xzt})F_{cc}\ ] - M_t{}^2[\lambda^3\chi a^2 s_{1u}\ F_{cs} + \lambda^4\mu a_x^2 c_{1u}F_{cc} - \lambda^6\chi s_{1u}(\ (a_x^2 I_{xxt} -$$
$$2a_x a_z I_{xzt} + a_z^2 I_{zzt}\ )\ )F_{cc}\ ] = 0 \quad (4.6)$$

This equation is the same as Eq. (25) of Ref. [2]. Similarly, the frequency equation of a uniform cantilever beam with a tip mass that is slender in the longitudinal direction that is derived by Bhat and Wagner [12] can be replicated by assuming only bending stiffness with negligible torsional deformation (i.e., $\chi \to 0$), with the following conditions: $a_y = a_z = 0$ and $I_{xxt} = I_{xzt} = 0$.

The characteristic (frequency) equation, Eq. (4.5), reduces to

$$F_{cfv} - \lambda^3 I_{zzt} F_{crv} - M_t \lambda \left(F_{csv} + 2\lambda a_x s_v s h_v + \lambda^2 a_x^2 F_{crv} - \lambda^3 I_{zzt} F_{ccv} \right) = 0 \qquad (4.7)$$

Chapter 5

5.0 Numerical Simulation and Discussion

The Characteristic (frequency) equation of a cantilever beam with rigid tip mass experiencing flexural-flexural-torsional coupling is solved for a beam with the following material properties and geometric parameters: Young's modulus E= 210 GPa., Poisson's ratio $\nu = 0.3$, Density $\rho = 7000$ kgm^{-3}, Cross-sectional area A= 100 mm^{-2}, Length L=5 m and Torsional constant $J = 7.0865\text{x}10^{-10}$ m^4. The torsional constant is computed from the formula [22]

$$J \approx b^3 h\left(\frac{1}{3} - \frac{64}{\pi^5}\frac{b}{h}\tanh\left(\frac{\pi h}{2b}\right)\right) \tag{5.1}$$

The results are compared with the results obtained from commercial finite element software ANSYS. The ANSYS results are based on 500 "BEAM4" elements. The results are tabulated in Table 1. It is observed that the ANSYS results are in excellent agreement (up to the fourth decimal place).

Parameters	Analysis Method	Non-dimensional natural frequency λ				
		λ1	λ2	λ3	λ4	λ5
$M_t = 0$	ANSYS	1.8751	3.7502	4.6941	7.8548	9.3882
$I_{xx} = I_{yy} = I_{zz} = 0$	Present	1.8751	3.7502	4.6941	7.8548	9.3882
$M_t = 0.5$	ANSYS	1.4200	2.8400	4.1112	7.1904	8.2223
$I_{xx} = I_{yy} = I_{zz} = 0$	Present	1.4200	2.8399	4.1111	7.1903	8.2223
$M_t = 0.5, I_{xx} = 0.2$	ANSYS	1.4200	1.5958	2.8400	4.1112	7.1904
$I_{yy} = I_{zz} = 0$	Present	1.4200	1.5958	2.8400	4.1111	7.1903
$M_t = 0.5, I_{yy} = 0.2$	ANSYS	1.4200	2.4975	4.1112	4.5663	7.1904
$I_{xx} = I_{zz} = 0$	Present	1.4200	2.4974	4.1111	4.5662	7.1903
$M_t = 0.5, I_{zz} = 0.2$	ANSYS	1.2487	2.2831	2.8400	5.0360	8.0591
$I_{xx} = I_{yy} = 0$	Present	1.2487	2.2831	2.8400	5.0360	8.0590
$M_t = 0.5, I_{xx} = 0.2$	ANSYS	1.2487	1.5958	2.2831	2.4975	34.5663
$I_{xx} = I_{zz} = 0.2$	Present	1.2487	1.5958	2.2831	2.4974	4.5662

Table 5.1: Validation of the analysis for $a_x = a_y = a_z = 0.0$, $\alpha = 0.5$, $\mu = 1.1902319 \times 10^{-3}$ and $\chi = 0.8780$

5.1 Effect of varying the offset on the natural frequency

The effect of varying the offsets is examined using the following parameters: $\alpha = 0.5$, $M_t = 0.5$ and $I_{xx} = I_{yy} = I_{zz} = 0.2$. When any two offsets are varying, the non-varying offset is set to zero. The results for varying a_y and a_z (with $a_x = 0$) are depicted in Fig. 5.1. It is observed that the natural frequency decreases with increasing a_y (a_z) values for given values of a_z (a_y).

The results obtained for varying a_z and a_x, on the one hand, and a_x and a_y, on the other hand, are respectively illustrated in Figs. 5.2 and 5.3.The natural frequency in both scenarios decreases with increasing a_z or a_y for a given value of a_x. The offset along the longitudinal axis of the beam a_x has no significant effect on the natural frequency for a given value of a_z or a_y.

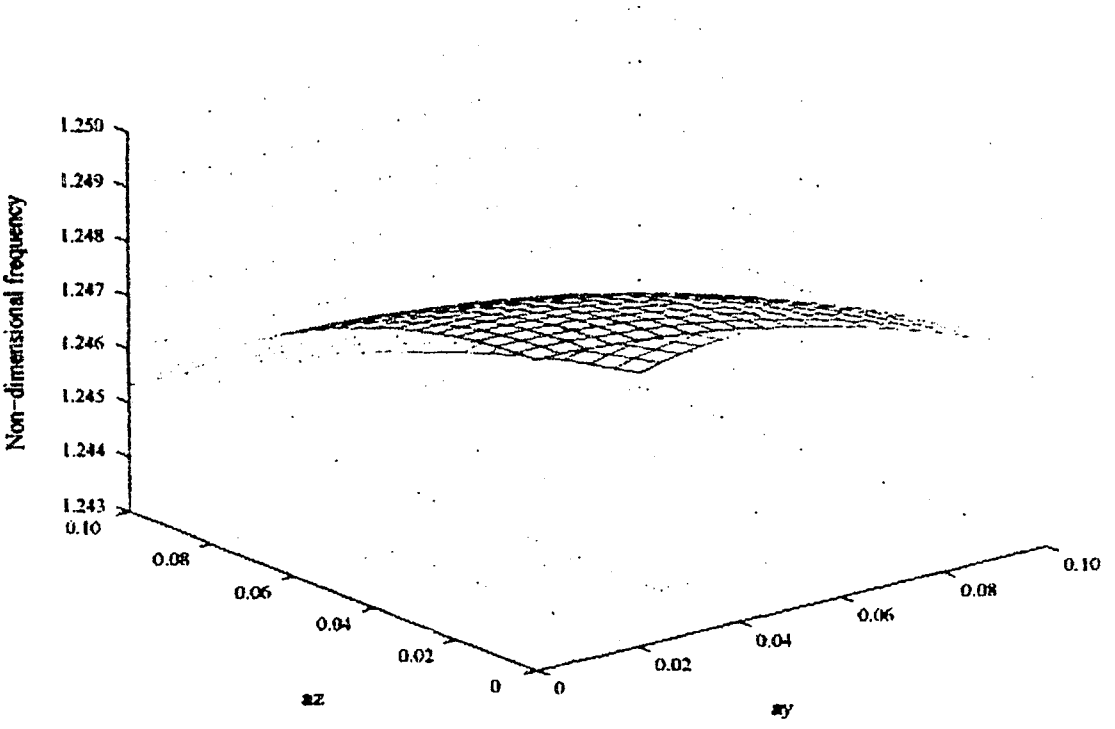

Fig. 5.1: Effect of varying the offset along the y-and z-axes for $\alpha = 0.5$, $M_t = 0.5$, $a_x = 0.0$.

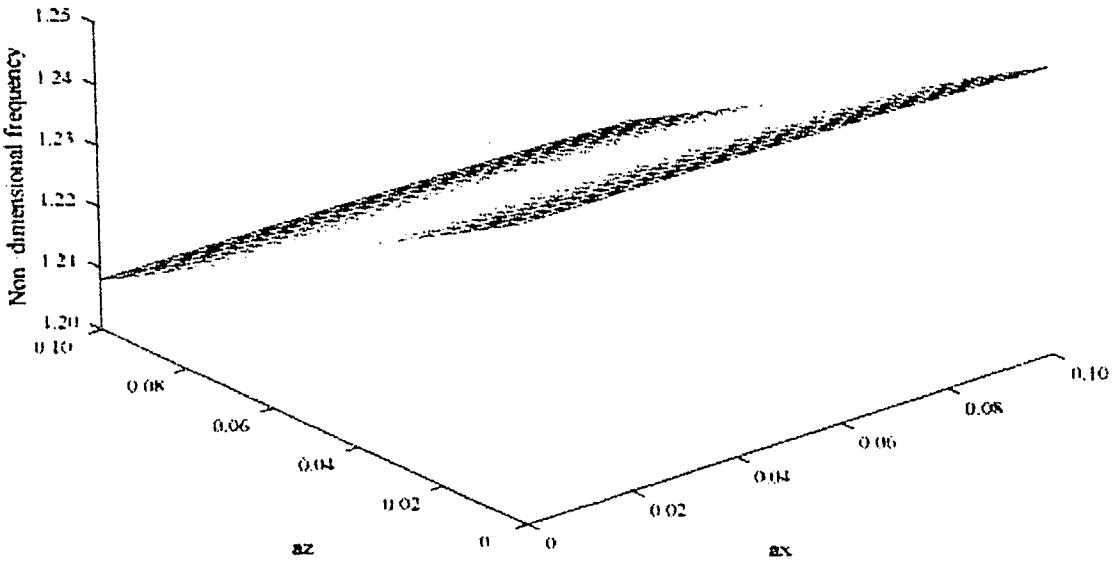

Fig. 5.2: Effect of varying the offset along the x-and z-axes for $\alpha = 0.5$, $M_t = 0.5$, $a_y = 0.0$.

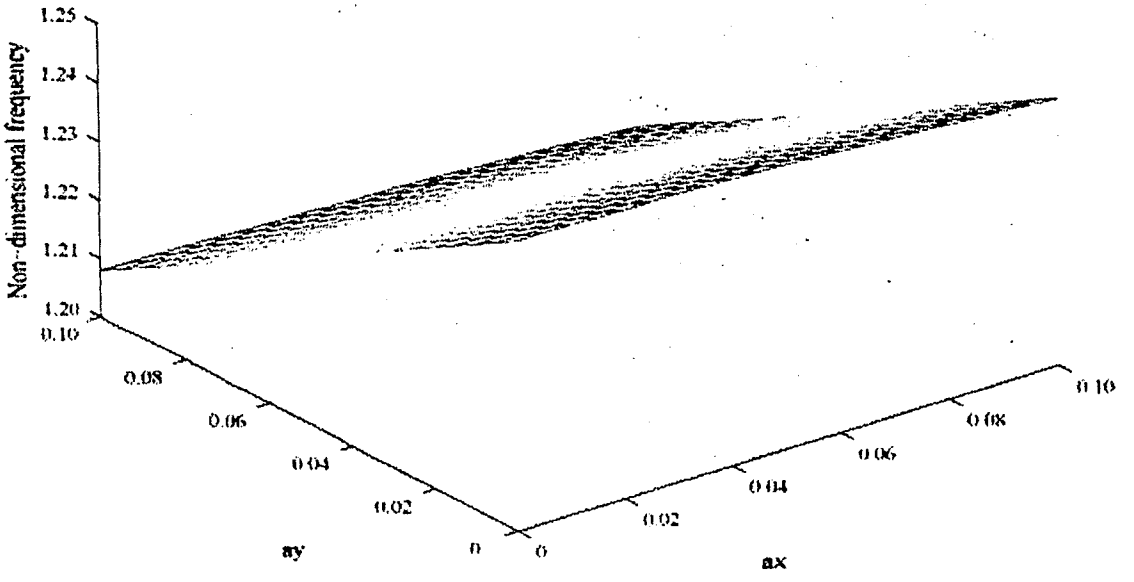

Fig.5.3: Effect of varying the offset along the x-and y-axes for $\alpha = 0.5$, $M_t = 0.5$, $a_z = 0.0$.

5.2 Effect of varying the moment of inertia on the natural frequency

The effect of varying the moment of inertia about the center of gravity is examined using the following parameters: $\alpha = 0.5, \chi = 8.7802 \times 10^{-1}, \mu = 1.1902319 \times 10^{-3}$, $a_x = 0.0$, $a_y = a_z = 0.05$ and $M_t = 0.5$. With I_{xx} fixed at 0.20, the results for varying I_{yy} and I_{zz} are illustrated in Fig. 5.4. The natural frequency decreases with increasing values of I_{zz} for given values of I_{yy}. The variations in I_{yy} do not, for the range of values examined, have any significant effect on the natural frequency for given values of I_{zz}.

The effect of varying I_{xx} and I_{zz} for $I_{yy} = 0.20$ (see Fig. 5.5) shows that the natural frequency decreases with increasing values of I_{zz} for a given value of I_{xx}. For a fixed I_{zz}, especially for higher values, the natural frequency is invariant for a range of I_{xx}. For small

fixed I_{zz} values, however, there is a range of I_{xx} over which the natural frequency is invariant, before decreasing with increasing I_{xx}.

The effect of varying I_{xx} and I_{yy} for $I_{zz} = 0.20$ is illustrated in Fig. 5.6. It is observed that for any given value of I_{yy}, there is a range of I_{xx} over which the natural frequency is invariant. Outside this range, the natural frequency decreases with increasing I_{xx}. The effect of varying I_{yy} for given I_{xx} is negligible.

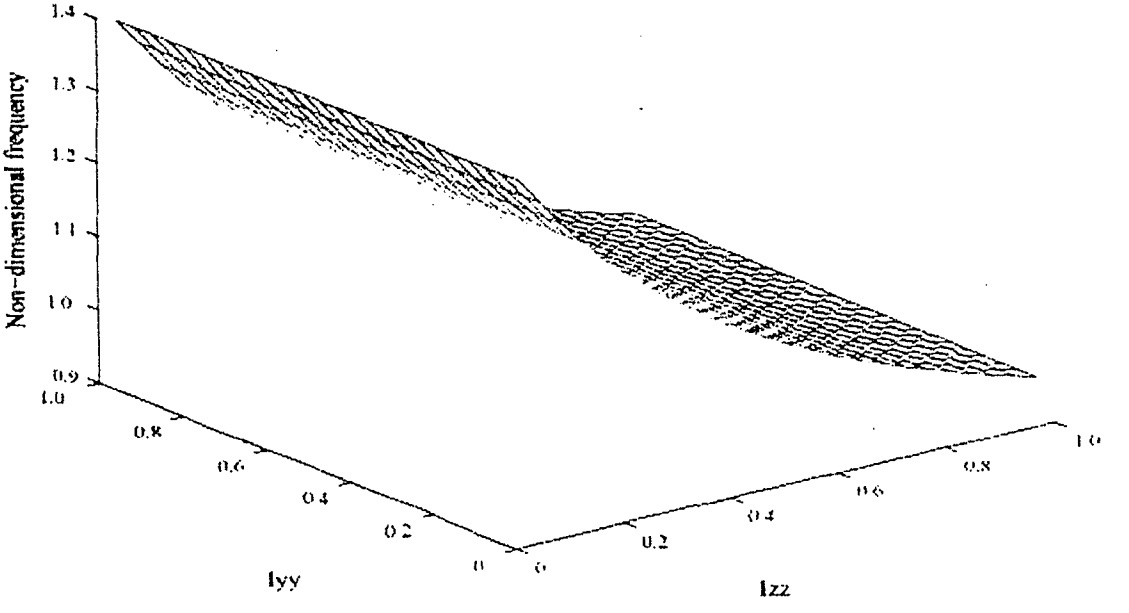

Fig. 5.4: Effect of varying the moments of inertia, I_{yy} *and* I_{zz} of the tip mass about its centre of gravity for $\alpha = 0.5, \chi = 8.7802 \times 10^{-1}, \mu = 1.1902319 \times 10^{-3}, I_{xx} = 0.20, a_x = 0.0,$ $a_y = a_z = 0.05$

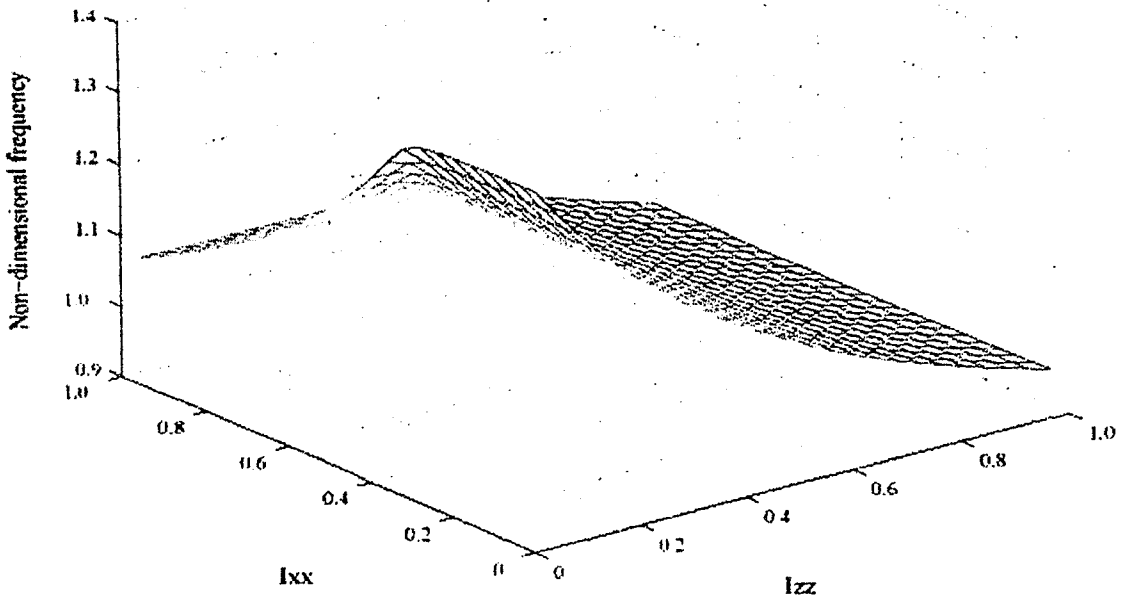

Fig. 5.5: Effect of varying the moments of inertia, I_{xx} *and* I_{zz} of the tip mass about its centre of gravity for $\alpha = 0.5, \chi = 8.7802 \times 10^{-1}, \mu = 1.1902319 \times 10^{-3}, I_{yy} = 0.20, a_x = 0.0,$ $a_y = a_z = 0.05$

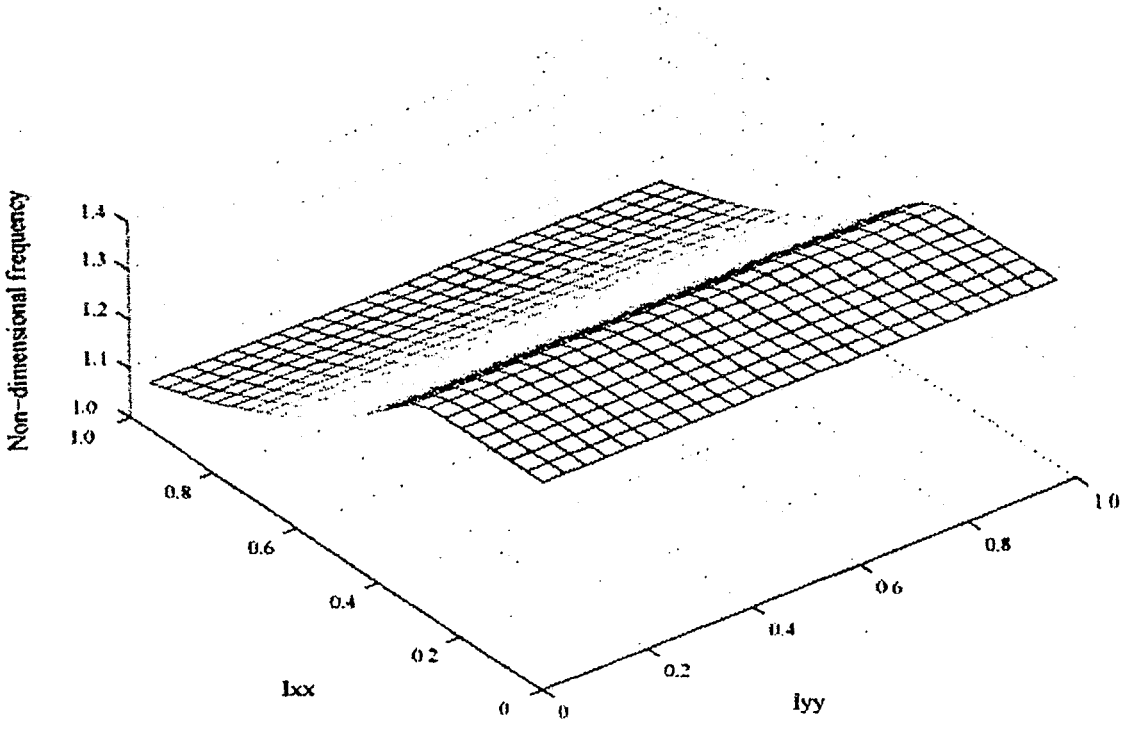

Fig. 5.6: Effect of varying the moments of inertia, I_{xx} *and* I_{yy} of the tip mass about its centre of gravity for $\alpha = 0.5, \chi = 8.7802 \times 10^{-1}, \mu = 1.1902319 \times 10^{-3}, I_{zz} = 0.20, a_x = 0.0,$ $a_y = a_z = 0.05$

5.3 Effect of payload mass on the natural frequency

The effect of varying the payload mass on the natural frequency is examined using the following parameters: $\alpha = 0.5, \chi = 8.7802 \times 10^{-1}$, $\mu = 1.1902319 \times 10^{-3}$, $I_{xx} = I_{yy} = I_{zz} = 0.20$. The non varying offsets are set equal to zero. Fig. 5.7-5.9 respectively illustrate the effects of varying the payload mass M_t with a_x, a_y or a_z. In all scenarios, the natural frequency is observed to decrease with increasing payload mass M_t, thus reflecting the increased system inertia. However, variations in a_x, a_y or a_z do not result in any significant change in the natural frequency. This could be because the extra inertia components are negligible.

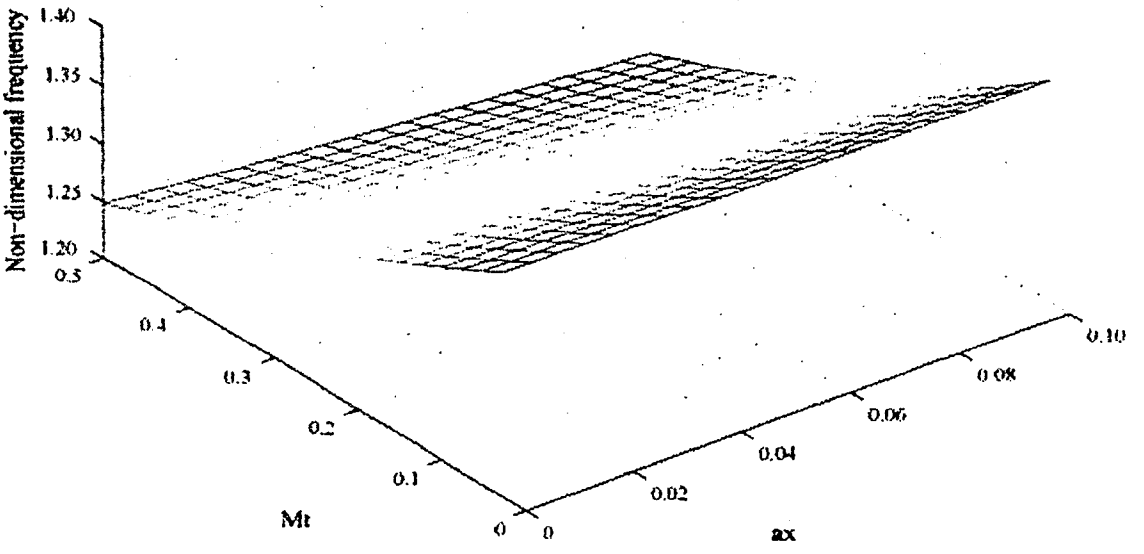

Fig. 5.7: Effect of varying the payload mass M_t and the offset about the x-axis a_x, for $\alpha = 0.5, \chi = 8.7802 \times 10^{-1}, \mu = 1.1902319 \times 10^{-3}, I_{xx} = I_{yy} = I_{zz} = 0.20,$ $a_y = a_z = 0.0$

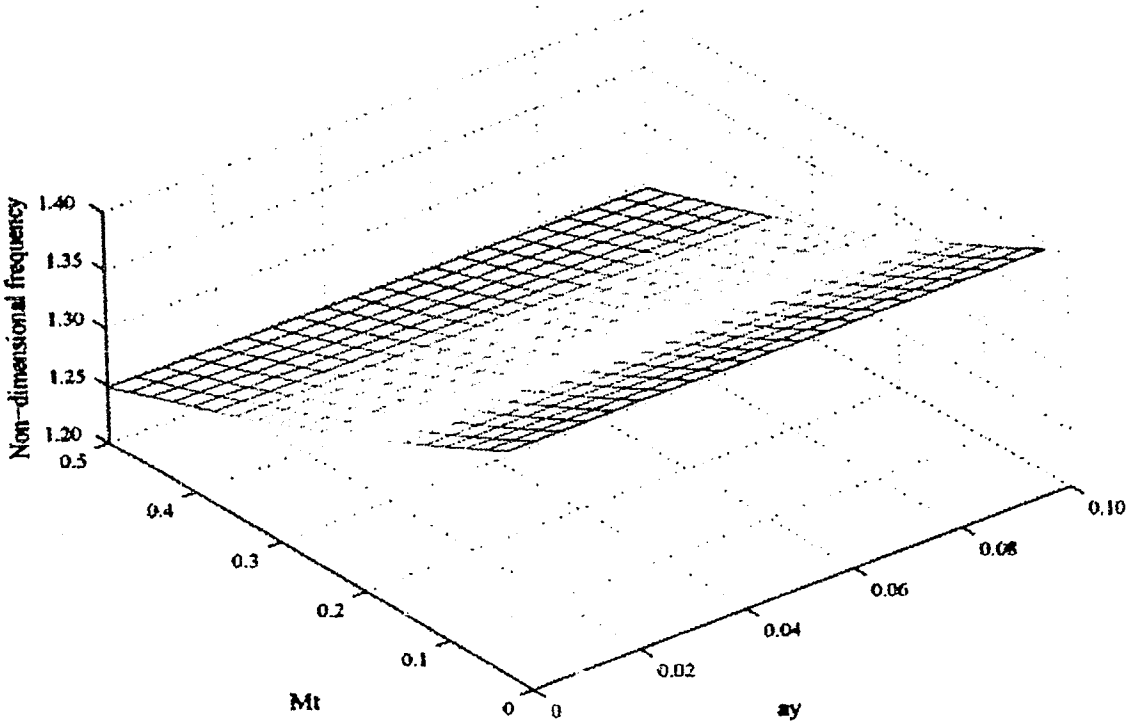

Fig. 5.8: Effect of varying the payload mass M_t and the offset about the y-axis a_y, for $\alpha = 0.5, \chi = 8.7802 \times 10^{-1}, \mu = 1.1902319 \times 10^{-3}, I_{xx} = I_{yy} = I_{zz} = 0.20$, $a_x = a_z = 0.0$

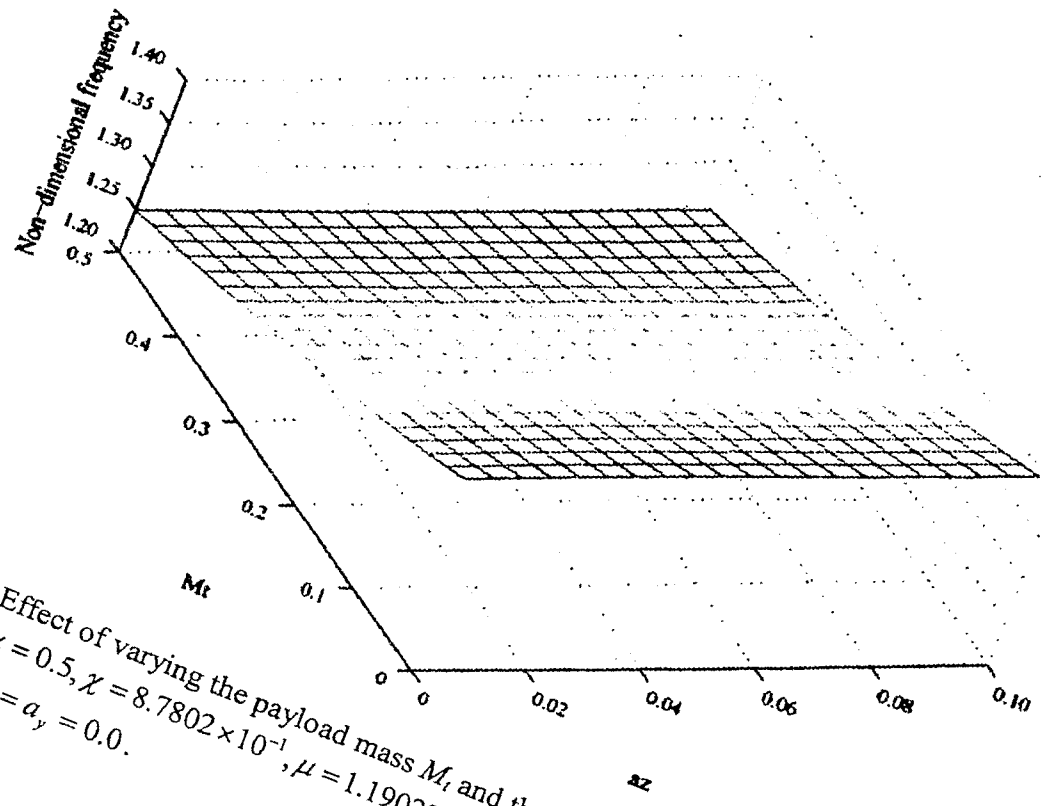

Fig. 5.9: Effect of varying the payload mass M_t and the offset about the z-axis a_z, for $\alpha = 0.5, \chi = 8.7802 \times 10^{-1}, \mu = 1.1902319 \times 10^{-3}, I_{xx} = I_{yy} = I_{zz} = 0.20,$ $a_x = a_y = 0.0.$

Chapter 6

6.0 Conclusion

The goal of this project is to calculate natural frequency of a manipulator which is modeled as a cantilever Euler-Bernoulli beam. The manipulator experiences torsional and bending deformation in XY and XZ planes. The analysis is restricted to small deformations, and Hamilton's principle is used to obtain the system governing equations. A closed form expression of the characteristic equation is derived, and this is solved by a root finding technique using a MATLAB computer program.

The effect of varying different parameters on the frequency equation of the system is observed. The accuracy of the frequency equation is supported by the results that are obtained from finite element software ANSYS. The ANSYS results are based on finite element analysis using 500 "BEAM4" elements and are in excellent agreement (up to the fourth decimal) with the present work. The possible extension to the project includes the use of other beam models and the inclusion of warping.

REFERENCES

[1] Love, A.E.H., A Treatise on the Mathematical Theory of Elasticity, Dover Publications Inc., New York; 1927.

[2] Oguamanam, D.C.D., Free vibration of beams with Finite mass rigid tip load and flexural-torsional coupling. International Journal of Mechanical Sciences 2003; 45: pp. 963-79.

[3] Strutt, J.W., Theory of Sound, Macmillan Publications, London; 1877.

[4] Timoshenko, S.P., History of Strength of Materials, Dover, New York; 1983.

[5] Timoshenko, S.P., On the correction for shear of the differential equation for transverse vibrations of prismatic bars, Philosophical Magazine and Journal of Science 1921; 41: pp. 744-7.

[6] Inman, D. J., Engineering vibration. Englewood Cliffs, NJ: Prentice-Hall; 1994.

[7] Shames, I. H. and Dym, C. L., Energy and Finite Element Methods in Structural Mechanics. Hemisphere Publishing Co; 1985.

[8] Goel, R.P., Vibrations of a beam carrying a concentrated. Journal of Applied Mechanics 1973; 40: pp. 821-2.

[9] Laura, P.A.A., Pombo, J.L. and Susemihl, E.A., A note on the vibrations of a clamped–free beam with a mass at the free end. Journal of Sound and Vibration 1974; 37: pp. 161-8.

[10] Bruch Jr. J.C. and Mitchell, T.P., Vibrations of mass-loaded clamped-free Timoshenko beam. Journal of Sound and Vibration 1987; 114: pp. 341-5.

[11] White, M.W.D. and Heppler, G.R., Vibration modes and frequencies of Timoshenko beams with attached rigid bodies. ASME Journal of Applied Mechanics 1995; 62: pp.193-9.

[12] Low, K.H., A note on the effect of hub inertia and payload on the vibration of a flexible slewing link. Journal of Sound and Vibration 1997; 204(5): pp. 823-8.

[13] Oguamanam, D.C.D., Hansen, J.S. and Heppler, G.R., Vibration of arbitrarily oriented two-member open frames with tip mass. Journal of Sound and Vibration 1998; 209: pp. 651-69.

[14] Bhat, B.R. and Wagner, H., Natural frequencies of a uniform cantilever with a tip mass slender in the longitudinal direction. Journal of Sound and Vibration 1976; 5(2): pp. 304-7.

[15] To, C.W.S., Vibration of a cantilever beam with a base excitation and tip mass. Journal of Sound and Vibration 1982; 83(4): pp. 445-60.

[16] Laura, P.A.A. and Gutierrez, R.H., Vibrations of an elastically restrained cantilever beam of varying cross section with tip mass of finite length. Journal of Sound and Vibration 1986; 108(1): pp. 123-31.

[17] Storch, J. and Gates, S., Transverse vibration and buckling of a cantilevered beam with the body under longitudinal acceleration. Journal of Sound and Vibration 1985; 99: pp. 43-52.

[18] Dokumaci, E., An exact solution for coupled bending and torsion vibrations of uniform beams having single cross-sectional symmetry, Journal of Sound and Vibration 1987; 119(3): pp. 443-9.

[19] Bishop, R. E. D., Cannon, S. M., and Miao, S., On Coupled Bending and Torsional Vibration of Uniform Beams, Journal of Sound and Vibration, 1989; 131(3): pp. 457-64.

[20] Kirk, C.L. and Wiedemann, S.M., Natural frequencies and mode shapes of a free–free beam with large end masses. Journal of Sound and Vibration 2002; 54(5): pp. 939-49.

[21] Oguamanam, D.C.D., Free vibration of manipulator with rigid tip mass: the case of flexural-flexural-torsional coupling: unpublished manuscript.

[22] Wang, C.T., Applied Elasticity. McGraw-Hill, New York; 1953.